UC Berkeley

UC Berkeley Previously Published Works

Title

NAIP-NLRC4 Inflammasomes Coordinate Intestinal Epithelial Cell Expulsion with Eicosanoid and IL-18 Release via Activation of Caspase-1 and -8

Permalink

https://escholarship.org/uc/item/3st853r8

Journal

Immunity, 46(4)

ISSN

1074-7613

Authors

Rauch, Isabella
Deets, Katherine A
Ji, Daisy X
et al.

Publication Date

2017-04-01

DOI

10.1016/j.immuni.2017.03.016

Peer reviewed

eScholarship.org Powered by the California Digital Library
University of California

Author Manuscript

Author Manuscript

Author Manuscript

Author Manuscript

HHS Public Access

Author manuscript

Immunity. Author manuscript; available in PMC 2018 April 18.

Published in final edited form as:

Immunity. 2017 April 18; 46(4): 649–659. doi:10.1016/j.immuni.2017.03.016.

NAIP-NLRC4 inflammasomes coordinate intestinal epithelial cell expulsion with eicosanoid and IL-18 release via activation of Caspase-1 and -8

Isabella Rauch[1], **Katherine A. Deets**[1], **Daisy X. Ji**[1], **Jakob von Moltke**[1,6], **Jeannette L. Tenthorey**[1], **Angus Y. Lee**[5], **Naomi H. Philip**[2], **Janelle S. Ayres**[1,7], **Igor E. Brodsky**[2], **Karsten Gronert**[3], and **Russell E. Vance**[1,4,5,8,*]

[1]Division of Immunology & Pathogenesis, Department of Molecular & Cell Biology, University of California, Berkeley 94720 USA

[2]Department of Pathobiology, University of Pennsylvania School of Veterinary Medicine, Philadelphia, PA 19104 USA

[3]Vision Science Program, School of Optometry, University of California at Berkeley, Berkeley, California 94720 USA

[4]Howard Hughes Medical Institute, University of California, Berkeley 94720 USA

[5]Cancer Research Laboratory and Immunotherapeutics and Vaccine Research Initiative, University of California, Berkeley 94720 USA

Summary

Intestinal epithelial cells (IECs) form a critical barrier against pathogen invasion. By generation of mice in which inflammasome expression is restricted to IECs, we describe a coordinated epithelium-intrinsic inflammasome response *in vivo*. This response was sufficient to protect against *Salmonella* tissue invasion, and involved a previously reported IEC expulsion that was coordinated with lipid mediator and cytokine production, and lytic IEC death. Excessive inflammasome activation in IECs was sufficient to result in diarrhea and pathology. Experiments with IEC organoids demonstrated that IEC expulsion did not require other cell types. IEC

*Correspondence: rvance@berkeley.edu.

[6]Current Address: Department of Immunology, University of Washington School of Medicine, Seattle, WA 98109 USA

[7]Current Address: Nomis Center for Immunobiology and Microbial Pathogenesis, The Salk Institute for Biological Studies, La Jolla, CA 92037, USA

[8]Lead contact.

Author contributions

I.R. and R.E.V. conceived the study, designed the experiments and wrote the paper; I.R. performed the majority of the experiments; K.A.D. helped with organoid experiments and infections; A.Y.L. performed Cas9 mRNA/ sgRNA injections into mouse zygotes; D.X.J. made *Gsdmd*$^{-/-}$ mice; J.L.T. performed co-immunoprecipitations; JvM cloned the construct for the iCASP1 mice and generated the iNLRC4 mice to initiate the study. J.S.A cloned the construct for the iNLRC4 mice.; I.E.B. and N.H.P. helped with *Ripk3*$^{-/-}$*Casp8*$^{-/-}$experiments; K.G. provided reagents and expertise for eicosanoid analysis. All authors discussed the results and commented on the manuscript.

The authors declare no competing financial interests.

Publisher's Disclaimer: This is a PDF file of an unedited manuscript that has been accepted for publication. As a service to our customers we are providing this early version of the manuscript. The manuscript will undergo copyediting, typesetting, and review of the resulting proof before it is published in its final citable form. Please note that during the production process errors may be discovered which could affect the content, and all legal disclaimers that apply to the journal pertain.

Author Manuscript Author Manuscript Author Manuscript Author Manuscript

expulsion was accompanied by a major actin rearrangement in neighboring cells that maintained epithelium integrity, but, did not absolutely require Caspase-1 or Gasdermin D. Analysis of *Casp1*$^{-/-}$*Casp8*$^{-/-}$ mice revealed a functional Caspase-8 inflammasome *in vivo*. Thus, a coordinated IEC-intrinsic, Caspase-1 and -8 inflammasome response plays a key role in intestinal immune defense and pathology.

Graphical Abstract

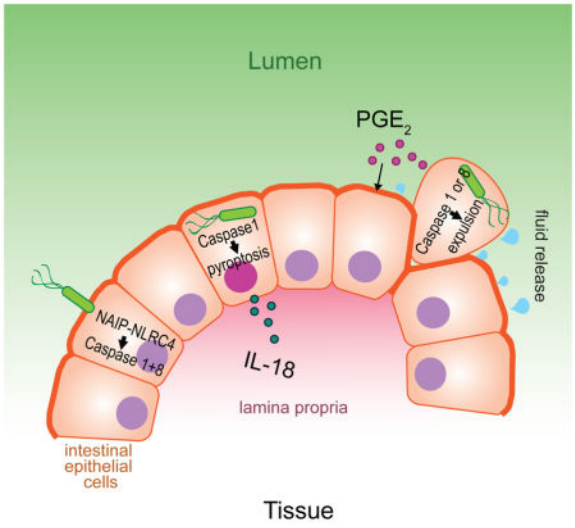

Introduction

Inflammasomes are cytosolic multi-protein complexes that initiate innate immune responses against invasive microbial pathogens by activating inflammatory caspases such as Caspase-1 (Lamkanfi and Dixit, 2014; Strowig et al., 2012). Although inflammasome components are broadly expressed, the role of inflammasomes has primarily been studied in hematopoietic cells. Studies of intestinal epithelial cells (IECs) suggest an epithelium-intrinsic role for the NLRP6 inflammasome in regulating inflammasome responses (Elinav et al., 2011; Levy et al., 2015; Sellin et al., 2015; Wlodarska et al., 2014), but whether NLRP6 itself forms an inflammasome or has other functions remains unclear (Anand et al., 2012). In addition, non-canonical human Caspase-4 and mouse Caspase-11 inflammasome activation has been implicated in epithelial responses upon infection (Knodler et al., 2014).

IECs also express NAIP-NLRC4 inflammasomes (Hu et al., 2010; Sellin et al., 2014). NAIP-NLRC4 inflammasomes are activated when bacterial protein ligands such as flagellin bind to NAIP family members, leading them to co-assemble with NLRC4 to form an inflammasome that activates Caspase-1 (Hu et al., 2015; Kofoed and Vance, 2011; Zhang et al., 2015; Zhao et al., 2011). Studies of human patients with gain-of-function *NLRC4* mutations suggest that NLRC4 activation can produce severe gut pathology, but whether this is due to hematopoietic or epithelial NLRC4 expression is unresolved (Canna et al., 2014; Romberg et al., 2014). *In vivo* studies of NLRC4-deficient animals demonstrated a role for NLRC4 in *Salmonella* infection (Broz et al., 2010; Carvalho et al., 2012; Franchi et al.,

Author Manuscript Author Manuscript Author Manuscript Author Manuscript

2012; Lara-Tejero et al., 2006; Mariathasan et al., 2004; Miao et al., 2010) and inflammation-induced colon cancer (Hu et al., 2010), but whether NLRC4 has an IEC-intrinsic function in these scenarios has not been addressed. Studies utilizing intestinal epithelium-specific NAIP deficient mice demonstrated an epithelium intrinsic requirement for NAIPs in *Salmonella* infection (Sellin et al., 2014) and colon tumorigenesis (Allam et al., 2015), but whether and/or how NLRC4 or Caspase-1 is involved remains unclear (Allam et al., 2015). A study using bone marrow transfer suggested NLRC4 in non-hematopoetic cells is protective in infection with the epithelial cell-adhering pathogen *Citrobacter rodentium* (Nordlander et al., 2013), but interpretation of bone-marrow chimeras is complicated by the possible presence of radioresistant hematopoietic cells. In macrophages, NAIP-NLRC4 activation results in Caspase-1 dependent processing and release of pro-inflammatory interleukins-1β and -18, and a lytic cell death called pyroptosis. By contrast, NAIP-NLRC4 activation in IECs was recently reported to result in their non-lytic expulsion into the gut lumen and protection from Salmonella invasion (Sellin et al., 2014). Why macrophages but not epithelial cells would undergo pyroptosis upon Caspase-1 activation is not clear. In addition, whether inflammasome-dependent expulsion is an epithelial cell type-intrinsic response, or whether it involves other cell types, has not been addressed.

In this study, we provide genetic evidence for a coordinated intestinal epithelial cell-intrinsic inflammasome response *in vivo*. We demonstrate that IEC-specific activation of the NLRC4 inflammasome was sufficient to result in the production of eicosanoid lipid mediators, cell death accompanied by membrane permeability, and rapid IEC expulsion from the epithelial layer. The IEC inflammasome response did not absolutely require Caspase-1 or Gasdermin D, the known signaling components downstream of NLRC4 (Ding et al., 2016; Kayagaki et al., 2015). By generation of mice doubly deficient in Caspase-1 and Caspase-8, we have implicated Caspase-8 in NLRC4 inflammasome responses *in vivo*.

Results

NLRC4 induces epithelium-intrinsic cell expulsion, fluid loss, and eicosanoid and IL-18 release

To study cell type-specific roles of NLRC4, we engineered *Nlrc4*$^{-/-}$ mice to re-express NLRC4 from the *Rosa26* locus under Cre-inducible control (iNLRC4 mice, Fig. 1A, Fig. S1A, S1B). In these mice, Cre excises a floxed transcriptional STOP cassette that is upstream of *Nlrc4*. An internal ribosome entry site (IRES)-GFP reporter inserted downstream of *Nlrc4* allows identification of cells in which the STOP cassette has been excised. Crossing iNLRC4 mice to a *Vil1-cre* or *Lyz2-cre* transgene resulted in mice in which NLRC4 and GFP are expressed selectively in Villin^{+} IECs or LysM^{+} hematopoietic cells (monocytes, macrophages, granulocytes), respectively. To activate NLRC4 in the absence of potentially confounding toll-like receptor (TLR) stimulation that accompanies bacterial infections, we used FlaTox, a previously described reagent for delivery of the NAIP5 ligand flagellin to the cytosol of cells (Ballard et al., 1996; Kofoed and Vance, 2011; Moltke et al., 2012; Rauch et al., 2016; Zhao et al., 2011). As reported previously (Moltke et al., 2012), systemic NAIP5-NLRC4 activation by FlaTox treatment of wild-type mice caused rapid hypothermia and vascular fluid loss, resulting in a marked increase in hematocrit,

Author Manuscript Author Manuscript Author Manuscript Author Manuscript

whereas *Nlrc4*$^{-/-}$ mice were fully protected from all symptoms (Fig. 1B, C). Consistent with the previously described role of peritoneal macrophages in this phenotype (Moltke et al., 2012), *Lyz2-cre*$^{+}$iNLRC4 mice succumbed to FlaTox with similar kinetics as wild-type mice. FlaTox treated *Vil1-cre*$^{+}$iNLRC4 mice that expressed NLRC4 only in IECs also experienced drastic hypothermia and a markedly increased hematocrit (Fig. 1B, C). Furthermore, these mice also exhibited diarrhea, in contrast to mice expressing NLRC4 only in LysM^{+} myeloid cells (Fig. 1D).

Eicosanoid lipid mediators, such as prostaglandins, can induce fluid loss and diarrhea, and are a major contributor to the pathology caused by FlaTox (Moltke et al., 2012). Therefore, we analyzed amounts of the prostaglandin PGE_2 in the intestinal tissue of our mice. Activation of NLRC4 onIy in IECs led to amounts of PGE_2 comparable to wild-type animals, demonstrating that inflammasome activation selectively in epithelial cells was sufficient to lead to local eicosanoid release (Fig. 1E). Specific activation of NLRC4 in IECs was also sufficient to produce significant systemic amounts of interleukin-18 (Fig. 1F), although NLRC4-mediated release of IL-18 by IECs was less than that released by myeloid cells (Fig. S1C). Intestinal tissue-derived IL-18 however seemed to be largely due to NLRC4 activation in epithelial cells (Fig. S1C).

Most dramatically, histological analysis of small intestines from *Vil1-cre*$^{+}$iNLRC4 mice 60 minutes after FlaTox injection showed a massive expulsion of IECs into the intestinal lumen, causing marked villus blunting. Despite severe IEC sloughing, the intestinal epithelial layer appeared to remain contiguous over large areas, especially at early timepoints, though breakdown was evident by 60 min (Fig. 1G). These results demonstrate that inflammasome activation selectively in epithelial cells is sufficient to result in a coordinated innate immune response involving eicosanoid and cytokine release, loss of fluid, and expulsion of IECs into the intestinal lumen.

Epithelial NLRC4 is sufficient to protect against intestinal *Salmonella* invasion

To determine whether the epithelium-intrinsic inflammasome response was sufficient to protect against an invasive bacterial pathogen, we infected iNLRC4 mice with *Salmonella enterica* serovar Typhimurium (*S.* Typhimurium) and analyzed early tissue colonization. Expression of NLRC4 selectively in IECs was sufficient to significantly reduce bacterial colonization of cecum tissue compared to *Nlrc4*$^{-/-}$ mice (Fig. 1H), whereas expression of NLRC4 selectively in myeloid cells had a minimal effect on cecum tissue colonization. Bacterial translocation to mesenteric lymph nodes, spleens and livers trended lower in mice expressing NLRC4 in myeloid as well as in epithelial cells, though this decrease was not statistically significant (Fig. S1D).

Inflammasome activation induces cell autonomous expulsion and lytic death of IECs

The above results demonstrated that NLRC4 activation selectively in intestinal epithelial cells was sufficient to induce pathology and protect against invasive bacterial pathogens, but did not address whether communication between epithelial cells and other cell types may also be involved in these responses. Therefore, to examine whether the NLRC4 inflammasome-induced cell expulsion of IECs is a cell type-intrinsic process, we generated

Author Manuscript Author Manuscript Author Manuscript Author Manuscript

intestinal epithelial stem cell-derived organoids (Miyoshi and Stappenbeck, 2013), and treated these organoids with FlaTox. Intestinal organoids consist of pure cultures of epithelial cells, thereby eliminating contributions from other cell types. The organoid system provided the further advantage of allowing us to visualize inflammasome-dependent epithelial cell expulsion using live cell imaging (Fig. 2A upper row, Movie S1, left). Activation of NLRC4 in organoids led to dramatic cell expulsion and collapse of the organoid. Organoids derived from intestinal stem cells of *Nlrc4*$^{-/-}$ mice did not exhibit IEC expulsion upon FlaTox treatment (Movie S2). IEC expulsion was a remarkably rapid process, requiring ~6 minutes to complete, and was always unidirectional, with cells expelled selectively into the organoid lumen. Importantly, we observed that cells became permeable to propidium iodide (PI), a dye excluded from intact cells, prior to expulsion. The early loss of plasma membrane integrity is characteristic of pyroptotic cell death and distinguishes inflammasome-driven epithelial cell expulsion from previously reported mechanisms of epithelial cell expulsion (Eisenhoffer et al., 2012; Rosenblatt et al., 2001). Indeed, organoids treated with tumor necrosis factor-α (TNF-α) to induce apoptosis resulted in expulsion of intact (PI-negative) cells (Fig. 2A lower row, B, Movie S1, right).

Our data suggest that inflammasome activation in IECs results in a loss of plasma membrane integrity and cell death that closely resembles pyroptotic cell death observed in macrophages (LaRock and Cookson, 2013). Our results differ from a previous report that concluded inflammasome activation in IECs does not result in pyroptosis (Sellin et al., 2014). However, this prior report assayed for plasma membrane integrity by observing whether tandem RFP protein is retained cytosolically in IECs. It is now appreciated that tandem RFP (60 kDa, (Campbell et al., 2002)) is likely too large to escape rapidly through the ~10–16nm Gasdermin D plasma membrane pores that form during pyroptosis (Aglietti et al., 2016; Ding et al., 2016). Also, in a *S.* Typhimurium infected epithelial cell line, Caspase-1 activation and uptake of a cell viability dye have been reported prior to cell extrusion (Knodler et al., 2010). Thus, to assess whether IECs undergo pyroptosis-like death prior to expulsion *in vivo*, we injected FlaTox-treated mice with PI and performed histological analysis of small intestinal tissue (Fig. 2C). Wild-type mice showed numerous PI^{+} cells in the epithelial layer, indicating that they have lost plasma membrane integrity prior to expulsion. As a negative control, we failed to find any PI^{+} IECs in *Nlrc4*$^{-/-}$ animals injected with FlaTox. We also examined colon tissue and colon derived organoids and obtained similar results (Fig. S2A, B). As further confirmation that inflammasome activation causes IECs to lose membrane integrity prior to expulsion, we examined leakage of GFP (26.9 kDa), which is co-expressed in IECs in our genetically targeted iNLRC4 mice and is small enough to escape through Gasdermin D pores. We found that PI^{+} cells showed significantly lower GFP intensity then their PI-negative neighbors, suggesting a loss of cytoplasmic GFP after inflammasome activation (Fig. 2D, E). Together these results show that NLRC4 inflammasome activation in intestinal epithelial cells leads to a lytic cell death, resembling pyroptosis, that is coordinated with IEC expulsion from the epithelial layer.

The apparent lysis of IECs while still within the intestinal epithelium might be expected to result in loss of the integrity of the epithelial layer, thereby compromising its important barrier function. However, we observed that a majority of IECs adjacent to the PI^{+} epithelial cells formed an actin ‘purse-string’ that appeared to effectively seal off the pyroptotic cell

Author Manuscript Author Manuscript Author Manuscript Author Manuscript

and ensure the continuity of the epithelial layer (Fig. 2C, F). Formation of a similar actin structure has been observed previously in extrusion of pre-apoptotic cells from epithelia (Rosenblatt et al., 2001), but its function may be particularly important during inflammasome-dependent IEC expulsion, since this appears to be accompanied by death of epithelial cells while still in the epithelial layer.

To ascertain the role of actin during IEC expulsion, we added cytochalasin D, an inhibitor of actin polymerization, to FlaTox treated organoids (Movie S3, left and 2G). Cells in cytochalasin D-treated organoids still became permeable to PI after FlaTox exposure, demonstrating that actin rearrangement is not required for pyroptosis of epithelial cells. However, these PI^+ (lysed) cells remained trapped in the epithelial monolayer and were not expelled. Similar results were obtained using jasplakinolide, an inhibitor of actin disassembly (Movie S3, right). Organoids treated with inhibitors only did not display any PI positive cells; however, they did exhibit some disorganization at later timepoints, probably because regular actin modifications are important for monolayer stability (not shown). Taken together, these results support the idea that rapid actin rearrangement is important to prevent loss of barrier integrity upon epithelial cell pyroptosis.

Caspase-1 is required for IEC pyroptosis but not IEC expulsion

In macrophages, Caspase-1 appears to be essential for NLRC4-induced pyroptosis and cytokine processing. In IECs, NLRC4-dependent IL-18 release also required Caspase-1 (Fig. 1F, Fig. S1C; *Casp1* singly-deficient mice generated by CRISPR/Cas9; Fig. S4A–C). However, Caspase-1 and -11-deficient mice nevertheless exhibited kinetically delayed hypothermia and hemoconcentration after injection with FlaTox (Moltke et al., 2012). These effects were accompanied by significant epithelial cell expulsion (Fig. 3A). The intestines of *Casp1*$^{-/-}$*Casp11*$^{-/-}$ mice injected with FlaTox and PI still showed the characteristic actin structures surrounding cells undergoing expulsion, however they did not exhibit any PI positive cells (Fig. 3A, B). Thus, NLRC4-dependent expulsion of IECs does not appear to require *Casp1*. To address the cell type-intrinsic function of *Casp1* in IECs, we generated inducible *Casp1* mice ('iCasp1 mice', analogous to iNLRC4 mice, see Fig. S3A–D) and crossed these mice to the *Vil1-cre* and *Lyz2-cre* transgenic lines. Upon FlaTox treatment, *Vil1-cre*$^+$iCasp1 mice show a more severe loss of body temperature, increase in hematocrit, diarrhea and tissue PGE_2 than *Casp1*$^{-/-}$Casp*11*$^{-/-}$ mice (Fig. 3C, Fig. S3E–G), indicating that Caspase-1 expression in epithelial cells is sufficient to mediate rapid IEC pyroptotic cell death and intestinal pathology. Accordingly, we found PI^+ IECs in the intestines of *Vil1-cre*$^+$iCasp1 mice after FlaTox injection (Fig. 3A, B). Similar to our observations in iNLRC4 mice, expression of Caspase-1 only in myeloid cells led to a phenotype similar to that seen in wildtype animals upon FlaTox injection (Fig. 3C, Fig. S3E–G). Confirming our *in vivo* observations, when we treated intestinal organoids derived from *Casp1*$^{-/-}$ mice with FlaTox, we observed IEC expulsion, but importantly, the IECs did not become PI^+ prior to expulsion, in contrast to wild-type IECs (compare Fig. 2A and 3D and supplemental Movie S1 and S4).

Gasdermin D is required for IEC pyroptosis but not IEC expulsion

Gasdermin D was recently identified as the main effector of pyroptosis downstream of Caspase-1 and -11 (Kayagaki et al., 2015; Shi et al., 2015). To determine whether *Gsdmd* is

Author Manuscript Author Manuscript Author Manuscript Author Manuscript

required for IEC pyroptosis-like death, we generated *Gsdmd*$^{-/-}$ mice using CRISPR/Cas9 (Fig. S4D–F). We observed that FlaTox did not induce epithelial pyroptosis in *Gsdmd*$^{-/-}$ mice (Fig. 4A, B). However, *Gsdmd*$^{-/-}$ mice were still susceptible to FlaTox, and exhibited robust epithelial cell expulsion, indicating that the *Casp1*-independent effects of NLRC4 inflammasome activation in epithelial cells do not require Gasdermin D (Fig. 4A, C, D; Fig. S4G, H). Therefore, IEC pyroptotic-like death requires *Casp1* and *Gsdmd*, but even in the absence of *Casp1* and *Gsdmd*, a delayed non-pyroptotic NLRC4-dependent IEC expulsion and intestinal pathology can still occur.

ASC is required for Caspase-1-independent NLRC4 signaling

Casp1$^{-/-}$*Casp11*$^{-/-}$ mice additionally deficient for the inflammasome adaptor ASC (encoded by the *Pycard* gene) were completely protected from hypothermia upon systemic NLRC4 activation (Fig. 5A). Phenocopying *Nlrc4*$^{-/-}$ mice, *Casp1*$^{-/-}$*Casp11*$^{-/-}$ *Pycard*$^{-/-}$ mice were also protected from the FlaTox-induced increase in hematocrit and PGE_2 as well as diarrhea (Fig. 5B, Fig. S3E–G) and epithelial cell expulsion (Fig. 5C). Loss of ASC alone did not confer any significant protection. Taken together, the above results suggest that NLRC4 activation in IECs can result in *Casp1*-dependent *Pycard*-independent pyroptosis, as well as a *Pycard*-dependent response which does not require *Casp1* and is sufficient to induce IEC expulsion and intestinal pathology.

A Caspase-8 inflammasome compensates for loss of Caspase-1

We sought to determine how NLRC4 induces IEC expulsion and intestinal pathology independent of *Casp1* and *Gsdmd*. Caspase-8 can bind the Pyrin domain of ASC (Masumoto et al., 2003) and has been reported to be recruited to the NLRC4 inflammasome ASC speck upon *Salmonella* infection of macrophages (Man et al., 2013). However, loss of *Casp8* did not affect cell death in this context, possibly because of compensation from *Casp1*. Caspase-8 has also been reported to function in NLRP3-induced IL-1β release (Antonopoulos et al., 2015; Karki et al., 2015). However, these experiments did not exclude the possibility that Caspase-8 is required for transcriptional priming upstream of NLRP3 or pro-IL-1β, rather than for signaling downstream of inflammasome activation (Antonopoulos et al., 2015; Gurung and Kanneganti, 2015; Karki et al., 2015; Man et al., 2013). In contrast to NLRP3, the NLRC4 inflammasome does not require transcriptional priming, and epithelial cell expulsion is a rapid, transcription-independent process. Thus, we sought to take advantage of our experimental system to establish a functional role for Caspase-8 downstream of NLRC4 inflammasome activation *in vivo*. Since loss of *Casp8* results in *Ripk3*-dependent embryonic lethality, we used CRISPR/Cas9 to create *Casp8*-deficient mice on a *Casp1*$^{-/-}$*Ripk3*$^{-/-}$ background (Fig. S5A, B). Remarkably, the *Casp1*$^{-/-}$*Casp8*$^{-/-}$*Ripk3*$^{-/-}$ mice were fully protected from FlaTox and phenocopied the complete resistance of *Nlrc4*$^{-/-}$ mice to inflammasome-induced hypothermia, hematocrit increase, diarrhea and IEC expulsion (Fig. 6A, B, Fig. S5C, D). By contrast, *Casp8*$^{-/-}$*Ripk3*$^{-/-}$, *Casp1*$^{-/-}$*Ripk3*$^{-/-}$ and *Ripk3*$^{-/-}$ mice exhibited robust FlaTox-induced pathology (Fig. 6A, B). Furthermore, *Casp8*$^{-/-}$*Ripk3*$^{-/-}$ organoids treated with Flatox showed expulsion of PI-permeable cells (Movie S5), demonstrating that while Caspase-1 is not essential to mediate the effects of NLRC4 activation in IECs, it is sufficient. Accordingly, organoids derived from *Casp1*$^{-/-}$*Casp8*$^{-/-}$*Ripk3*$^{-/-}$ mice were completely

Author Manuscript Author Manuscript Author Manuscript Author Manuscript

protected from NLRC4 induced epithelial cell expulsion (Movie S6). PGE_2 amounts in intestines of *Ripk3*$^{-/-}$*Casp8*$^{-/-}$ mice injected with FlaTox were not decreased compared to controls (Fig. 6C). There was, however, an apparent (but not statistically significant) decrease of PGE_2 in *Ripk3*$^{-/-}$*Casp1*$^{-/-}$ intestines, and a further statistically significant decrease in *Casp1*$^{-/-}$*Casp8*$^{-/-}$*Ripk3*$^{-/-}$ tissue as compared to *Ripk3*$^{-/-}$ controls (Fig. 6C). Thus, both Casp1 and Casp8 contribute to the coordinated production of eicosanoids that accompany IEC expulsion downstream of NLRC4 activation. To further address cell type specificity of this response we treated organoids with FlaTox *in vitro* and analyzed supernatants for PGE_2 (Fig. S5E). All organoids except *Nlrc4*$^{-/-}$ and *Casp1*$^{-/-}$*Casp8*$^{-/-}$organoids released significant amounts of PGE_2 over background, confirming that the eicosanoid pathway is cell autonomously active in IECs.

As an additional approach to establish cell-type specific roles of Caspase-1 and -8, we generated bone marrow chimeras in which *Casp1*$^{-/-}$*Casp8*$^{-/-}$*Ripk3*$^{-/-}$ bone marrow was used to reconstitute *Casp1*$^{-/-}$*Casp11*$^{-/-}$ hosts. In these chimeras, the only functional NLRC4-activated caspase is Caspase-8 in IECs. The chimeras showed a robust hypothermic, hematocrit and diarrhea response to FlaTox, only marginally less than the response of control chimeras in which *Casp1*$^{-/-}$*Casp11*$^{-/-}$ mice were reconstituted *Ripk3*$^{-/-}$*Casp1*$^{-/-}$ bone marrow (in which Casp8 is present in both hematopoietic and non-hematopoietic cells). These results suggest that Caspase-8 functions in radioresistant cells *in vivo* (Fig. S5F, G, H).

Because radiation chimeras contain numerous radioresistant cells, potentially including radioresistant hematopoietic cells, the above bone marrow chimera experiment does not demonstrate that Caspase-8 functions in IECs. To address whether Caspase-8 is activated in IECs *in vivo*, we performed immunohistochemistry to detect cleaved Caspase-8. Intestines of FlaTox-injected wildtype and *Casp1*$^{-/-}$ mice showed cleaved Caspase-8 “specks”, which were absent from intestines of FlaTox-treated *Nlrc4*$^{-/-}$, *Casp8*$^{-/-}$, or *Pycard*$^{-/-}$ animals (Fig. S6 A, B). Furthermore, using a reconstituted inflammasome system with epitope-tagged proteins expressed in 293T cells, we found that Caspase-8 co-immunoprecipitated with NLRC4 and NAIP5 only in the presence of ASC (Fig. S6C). Thus, taken together, our genetic, cell biological, and biochemical data strongly demonstrate that a functional NLRC4-Casp8 inflammasome is operational in IECs *in vivo*.

Finally, to ascertain a function for the NLRC4-Casp8 inflammasome in host defense, we infected *Casp1*$^{-/-}$*Ripk3*$^{-/-}$ mice with *S*. Typhimurium. Although these mice were susceptible compared to wildtype or *Ripk3*$^{-/-}$ mice, they showed significantly lower tissue colonization than *Nlrc4*$^{-/-}$ animals (Figure 6D). This protection was lost upon additional deficiency of *Casp8*, as *Casp1*$^{-/-}$*Casp8*$^{-/-}$*Ripk3*$^{-/-}$ mice showed comparable tissue bacterial loads to *Nlrc4*$^{-/-}$ mice. These results demonstrate that in intestinal infections, Caspase-1 and -8 are activated downstream of NLRC4 to protect from pathogen invasion.

Discussion

By generating mice in which expression of inflammasome components is restricted to intestinal epithelial cells, our results identify a unique and coordinated cell-type intrinsic

Author Manuscript Author Manuscript Author Manuscript Author Manuscript

response of IECs upon NLRC4-Caspase-1 and/or Caspase-8 inflammasome activation *in vivo*. We have shown the NLRC4-induced response involves a *Casp1* and *Gsdmd*-dependent pyroptosis-like loss of epithelial cell plasma membrane integrity. This cell death was coordinated with a rapid expulsion of the pyroptotic IEC from the epithelial layer, a process that we showed was epithelial cell-intrinsic. IEC expulsion appears to play an important role in limiting bacterial penetration into deeper tissues (Sellin et al., 2014) (Fig. 1H). We also showed that IEC expulsion was coordinated with epithelial cell production of IL-18 as well as of eicosanoid lipid mediators such as PGE_2 that trigger vascular leakage and fluid accumulation in the intestinal lumen. We propose that the eicosanoid-induced fluid response acts in concert with IEC expulsion, providing a mechanism in which expelled infected cells can be flushed from the intestines. The released IL-18 is likely critical to recruit immune cells that prevent dissemination of bacteria that managed to traverse the epithelium at later timepoints (Müller et al., 2016). Importantly, at moderate, physiologically relevant amounts, controlled permeabilization and expulsion of epithelial cells does not appear to result in overt destruction of the epithelium. Instead, we found that neighboring epithelial cells rapidly rearranged their actin cytoskeleton to accommodate the loss of the expulsed cell. Importantly, we provide genetic evidence that a *Casp8*-dependent inflammasome response can also mediate IEC expulsion, eicosanoid release, and protection from pathogen invasion, even in the absence of *Casp1*. Unlike previous studies, our results are not likely confounded by the effects of Caspase-8-deficiency on transcription, as our use of FlaTox allows us to selectively activate NLRC4, and NLRC4 activation does not require transcriptional priming. We speculate that the alternative NLRC4- and Caspase-8-dependent pathway might be important to provide resistance to bacterial pathogens that inhibit Caspase-1. Thus, taken together, our results define how inflammasome activation leads to a multi-faceted and coordinated epithelial cell response — involving cell death, expulsion, eicosanoid release and actin remodeling — that is sufficient to provide protection from an invasive bacterial pathogen such as *Salmonella*. However, we also demonstrate that if this coordinated response is activated excessively, it can lead to major epithelial destruction and systemic pathology. We propose that the coordinated NLRC4-dependent response of epithelial cells likely contributes to intestinal pathology in humans with NLRC4 gain-of-function mutations (Canna et al., 2014; Romberg et al., 2014), and possibly other inflammatory bowel diseases as well.

Experimental procedures

Mouse experiments

All mice used were specific pathogen free, maintained under a 12-h light-dark cycle (7 a.m. to 7 p.m.) and given a standard chow diet (Harlan irradiated laboratory animal diet) *ad libitum*. Wild-type C57BL/6J mice were originally obtained from the Jackson Laboratories, *Nlrc4*$^{-/-}$ animals were from V. Dixit (Genentech, CA) (Mariathasan et al., 2004), *Casp1*$^{-/-}$*Casp11*$^{-/-}$ mice were provided by A. Van der Velden and M. Starnbach (Li et al., 1995) and *Ripk3*$^{-/-}$ mice were originally from Xiaodong Wang (He et al., 2009) and backcrossed to C57BL/6 by Astar Winoto. CRISPR/Cas9 targeting was performed by pronuclear injection of Cas9 mRNA and sgRNA into fertilized zygotes from colony born mice, essentially as described previously (Wang et al., 2013).

Author Manuscript Author Manuscript Author Manuscript Author Manuscript

Casp8$^{-/-}$*Ripk3*$^{-/-}$*Casp1*$^{-/-}$mice were generated by targeting *Casp8* using CRISPR-Cas9 in *Casp1*$^{-/-}$*Ripk3*$^{-/-}$ mice. Founder mice were genotyped as described below, and founders carrying mutations were bred one generation to C57BL/6J to separate modified haplotypes. Homozygous lines were generated by interbreeding heterozygotes carrying matched haplotypes. iNLRC4 and iCasp1 mice were generated by targeting the *Rosa26* locus for genomic insertion of a construct encoding a loxP-flanked transcriptional STOP cassette (Srinivas et al., 2001) upstream of the *Nlrc4* or *Casp1* cDNA transgene in JM8.F6 ES cells. An IRES–GFP (Sasaki et al., 2006) was included downstream of the *Nlrc4* cDNA to mark cells in which the STOP cassette has been excised. Founders were crossed to the respective gene deficient background (i.e., *Nlrc4*$^{-/-}$ or *Casp1*$^{-/-}$ *Casp11*$^{-/-}$) and then further to *Vil1-cre* (Jax strain 004586) or *Lyz2-cre* (Jax strain: 004781) transgenic lines. For bone marrow chimeras, mice were irradiated first with 500 and then 400 rad 4 h apart and reconstituted with 5×10^6 donor cells by retrorbital injection. Chimaeric mice were assayed 7 weeks after irradiation. Animals used in infection and FlaTox injection experiments were littermates or, if not possible, cohoused upon weaning (see figure legends). All animal experiments complied with the regulatory standards of, and were approved by, the University of California Berkeley Institutional Animal Care and Use Committee.

Toxins

Recombinant proteins (PA, LFn–flagellin (*L. pneumophila* flagellin (FlaA; accession YP_095369)), LFn-Fla166 (C-terminal 166 amino acids of FlaA) were purified from insect cells. His_6-LFn fused to the N-terminus of the indicated gene (Ser-Thr-Arg linker) or His_6-PA were cloned into pFastBacDual (Life Technologies) using the SalI and NotI restriction sites. Recombinant bacmids were generated to infect Sf9 cells according to the manufacturer's instruction. After 72hr of infection with P2 baculovirus, insect cells were lysed with buffered detergent (1% NP-40 in 20mM Tris, 150mM NaCl, pH 8.0) and then clarified by centrifugation at 50,000 x *g* for 45 min at 4ºC. Proteins were purified using Ni-NTA agarose (Qiagen), eluted with 500mM imidazole in 20mM Tris, 500mM NaCl, pH 8.0, then dialyzed into 20mM Tris, pH 8.0 and subjected to anion exchange chromatography (ENrich Q column, BioRad) using a gradient elution into high-salt buffer (20mM Tris, 1M NaCl, pH 8.0). Fractions containing protein were concentrated using Amicon-Ultra centrifugal filters (EMD Millipore) and quantified using a BCA kit (Fisher Scientific). Endotoxin contamination of the preparations (determined using a LAL chromogenic endotoxin quantitation kit (Pierce)) was estimated to result in application of approximately 0.4 ng/mouse of endotoxin, an amount below the threshold for systemic responses in mice (Copeland et al., 2005).

Toxin doses were 0.2–0.8μg/g body weight of PA combined with 0.1–0.4μg/g LFn-Fla, or 20–80ng/g LFnFla166 for intravenous (retro-orbital) delivery, or 16μg/ml of PA combined with 1μg/ml LFn-Fla166, for *in vitro* experiments. Rectal temperature was determined using a MicroTherma 2T thermometer (Braintree Scientific). Blood for hematocrit was collected by retroorbital bleed into StatSpin microhematocrit tubes (Fisher Scientific). For wet/dry ratio determination of intestinal contents, the content of the small intestine was placed into a tube, weighed, dried overnight in a 70C incubator and weighed again. For *in vivo* propidium

Author Manuscript Author Manuscript Author Manuscript Author Manuscript

iodide staining, mice were injected with 100μg/mouse propidium iodide intravenously (retro-orbital) 10 minutes before sacrifice.

Salmonella infections

Salmonella Typhimurium infections were performed as previously described (Barthel et al., 2003). Briefly, 7- to 12-week-old mice deprived of food and water for 4h were gavaged with 25 mg streptomycin sulfate. 24h later, mice again deprived of food and water for 4h were gavaged with 3×10^7 CFUs *S.*Tm SL1344. Cecum tissue was incubated in PBS/400 mg/ml gentamycin for 30 min to kill extra-tissue bacteria and washed 6 times in PBS. Cecum and MLN were homogenized in sterile PBS and plated on MacConkey agar containing 50 mg/ml streptomycin.

Eicosanoid analysis

To analyze PGE_2 tissue content using PGE2 EIA (Chayman chemicals) 100mg of snap frozen jejunum were homogenized in 1ml phosphate buffer (0.1 M phosphate, pH 7.4, containing 1 mM EDTA and 10 μM indomethacin) and prostaglandins were extracted as recommended by the manufacturer. Briefly, proteins were precipitated with 4ml ethanol followed by centrifugation at 3,000 x g for 10 min. Ethanol was evaporated under nitrogen and samples resuspended in ultrapure water and acidified to pH 4.0 with 1 M acetate buffer. Samples were applied to a methanol rinsed C-18 column, washed and eluted with 5 ml ethyl acetate containing 1% methanol. The ethyl acetate was evaporated under a stream of nitrogen and samples resuspended in 500 μl EIA Buffer. EIA was performed according to manufacturer's instructions. PGE_2 amounts were normalized to protein content of the original sample, determined by BCA assay.

ELISA

Mice were bled retroorbitaly and serum analyzed by ELISA using paired IL- 18 Abs (BD Biosciences and eBioscience). For tissue cytokine amounts snap frozen intestinal tissue was homogenized in PBS containing proteinase inhibitors (Pierce), spun at 18.000g and supernatants used for ELISA. Recombinant IL-18 (eBioscience) was used as a standard.

Histology and Histochemistry

For hematoxylin and eosin stainings, intact intestinal tissue was fixed for 24h in methacarn to preserve mucus and epithelial cells trapped inside the mucus. Tissue was paraffin embedded in a water free procedure, cut to 5μm and stained. For analysis of cleaved Caspase 8, GFP, propidium iodide and actin, intestinal tissue was sliced open and fixed in PLP buffer (0.05 M phosphate buffer containing 0.1 M L-lysine, pH 7.4, 2 mg/ml NaIO4 and 1%PFA). After fixation overnight, tissue was washed in phosphate buffer and immersed in 30% sucrose overnight. Tissue was frozen in OCT, cut and stained with 100nM actistain 488 phalloidin (cytoskeleton) followed by DAPI. For cleaved Caspase 8 staining, slides were blocked using 10% normal donkey serum in 0.1% Tween20, 100mMTrisHCl, 150mMNaCl, 0.5% blocking reagent (Perkin Elmer) for 30 minutes. Slides were stained with 1:400 rabbit anti-mouse cleaved caspase-8 (no. 8592; Cell Signaling Technology) for 60 followed by donkey anti rabbit alexa fluor 488 (JacksonImmunoReasearch) for 30 minutes, followed by

Author Manuscript Author Manuscript Author Manuscript Author Manuscript

DAPI. Slides were analyzed on a Zeiss LSM710 and GFP intensity was measured using imageJ software.

Organoids

Organoids from mouse small intestine were isolated and grown as previously described (Miyoshi and Stappenbeck, 2013). For live imaging, organoids were split into 8 well coverslides and 2 days after seeding preincubated with 100μg/ml propidium iodide in growth medium for 30 minutes before treatment with Fla166Tox or TNFα in growth medium containing 100μg/ml propidium iodide. For cytochalasin D treatment, organoids were incubated with FlaTox and 2.5μM cytochalasin D was added 10 minutes later. For jasplakinolide treatment, 8μM jasplakinolide was added at the same time as FlaTox. Live imaging was performed in an incubation chamber using a Nikon Widefield Epifluorescent Microscope. For eicosanoid measurements, organoids were differentiated as in (Sato and Clevers, 2013) with addition of 20 ng/ml IL-4 from day 3 on. On day 7, organoids were harvested in DPBS, seeded in 96- well plates and treated with FlaTox. Supernatants were analyzed after 2h.

Supplementary Material

Refer to Web version on PubMed Central for supplementary material.

Acknowledgments

We acknowledge the assistance of the UC Berkeley CRL Flow Cytometry Laboratory, Eric Chen, Peter Dietzen, Roberto Chavez, Jake Wu and James Kang for technical support, the Vance and Barton Labs for discussions, and Greg Barton for comments on the manuscript. We thank Xiaodong Wang for *Ripk3*$^{-/-}$ mice and the Winoto Lab for backcrossing the mice to the C57BL/6 background. This work was supported by the HHMI and NIH grants to R.E.V. (AI075039, AI063302) and NIH Grant (EY026082) to K.G.. R.E.V. was a Burroughs Wellcome Fund Investigator in the Pathogenesis of Infectious Disease and is an Investigator of the Howard Hughes Medical Institute. Research reported in this publication was supported in part by the National Institutes of Health S10 program under award number 1S10RR026866-01. The content is solely the responsibility of the authors and does not necessarily represent the official views of the National Institutes of Health. I.R. is supported by the Austrian Science Fund (FWF) (the Erwin Schrödinger Fellowship J3789-B22).

References

Aglietti RA, Estevez A, Gupta A, Ramirez MG, Liu PS, Kayagaki N, Ciferri C, Dixit VM, Dueber EC. GsdmD p30 elicited by caspase-11 during pyroptosis forms pores in membranes. Proc Natl Acad Sci USA. 2016; 113(28):7858–63. [PubMed: 27339137]

Allam R, Maillard MH, Tardivel A, Chennupati V, Bega H, Yu CW, Velin D, Schneider P, Maslowski KM. Epithelial NAIPs protect against colonic tumorigenesis. J Exp Med. 2015; 212:369–383. [PubMed: 25732303]

Anand PK, Malireddi RKS, Lukens JR, Vogel P, Bertin J, Lamkanfi M, Kanneganti TD. NLRP6 negatively regulates innate immunity and host defence against bacterial pathogens. Nature. 2012; 488:389–393. [PubMed: 22763455]

Antonopoulos C, Russo HM, El-Sanadi C, Martin BN, Li X, Kaiser WJ, Mocarski ES, Dubyak GR. Caspase-8 as an Effector and Regulator of NLRP3 Inflammasome Signaling. J Biol Chem. 2015; 290:20167–20184. [PubMed: 26100631]

Ballard JD, Collier RJ, Starnbach MN. Anthrax toxin-mediated delivery of a cytotoxic T-cell epitope in vivo. Proc Natl Acad Sci USA. 1996; 93:12531–12534. [PubMed: 8901616]

Barthel M, Hapfelmeier S, Quintanilla-Martínez L, Kremer M, Rohde M, Hogardt M, Pfeffer K, Rüssmann H, Hardt WD. Pretreatment of mice with streptomycin provides a Salmonella enterica

Author Manuscript Author Manuscript Author Manuscript Author Manuscript

serovar Typhimurium colitis model that allows analysis of both pathogen and host. Infect Immun. 2003; 71:2839–2858. [PubMed: 12704158]

Broz P, Newton K, Lamkanfi M, Mariathasan S, Dixit VM, Monack DM. Redundant roles for inflammasome receptors NLRP3 and NLRC4 in host defense against Salmonella. J Exp Med. 2010; 207:1745–1755. [PubMed: 20603313]

Campbell RE, Tour O, Palmer AE, Steinbach PA, Baird GS, Zacharias DA, Tsien RY. A monomeric red fluorescent protein. Proc Natl Acad Sci USA. 2002; 99:7877–7882. [PubMed: 12060735]

Canna SW, de Jesus AA, Gouni S, Brooks SR, Marrero B, Liu Y, DiMattia MA, Zaal KJM, Sanchez GAM, Kim H, et al. An activating NLRC4 inflammasome mutation causes autoinflammation with recurrent macrophage activation syndrome. Nat Genet. 2014; 46:1140–1146. [PubMed: 25217959]

Carvalho FA, Nalbantoglu I, Aitken JD, Uchiyama R, Su Y, Doho GH, Vijay-Kumar M, Gewirtz AT. Cytosolic flagellin receptor NLRC4 protects mice against mucosal and systemic challenges. Mucosal Immunol. 2012; 5:288–298. [PubMed: 22318495]

Copeland S, Warren HS, Lowry SF, Calvano SE, Remick D. Inflammation and the Host Response to Injury Investigators. Acute inflammatory response to endotoxin in mice and humans. Clin Diagn Lab Immunol. 2005; 12:60–67. [PubMed: 15642986]

Ding J, Wang K, Liu W, She Y, Sun Q, Shi J, Sun H, Wang D-C, Shao F. Pore-forming activity and structural autoinhibition of the gasdermin family. Nature. 2016

Eisenhoffer GT, Loftus PD, Yoshigi M, Otsuna H, Chien CB, Morcos PA, Rosenblatt J. Crowding induces live cell extrusion to maintain homeostatic cell numbers in epithelia. Nature. 2012; 484:546–549. [PubMed: 22504183]

Elinav E, Strowig T, Kau AL, Henao-Mejia J, Thaiss CA, Booth CJ, Peaper DR, Bertin J, Eisenbarth SC, Gordon, et al. NLRP6 inflammasome regulates colonic microbial ecology and risk for colitis. Cell. 2011; 145:745–757. [PubMed: 21565393]

Franchi L, Kamada N, Nakamura Y, Burberry A, Kuffa P, Suzuki S, Shaw MH, Kim YG, Núñez G. NLRC4-driven production of IL-1β discriminates between pathogenic and commensal bacteria and promotes host intestinal defense. Nat Immunol. 2012; 13:449–456. [PubMed: 22484733]

Gurung P, Kanneganti TD. Novel roles for caspase-8 in IL-1β and inflammasome regulation. Am J Pathol. 2015; 185:17–25. [PubMed: 25451151]

He S, Wang L, Miao L, Wang T, Du F, Zhao L, Wang X. Receptor interacting protein kinase-3 determines cellular necrotic response to TNF-alpha. Cell. 2009; 137:1100–1111. [PubMed: 19524512]

Hu B, Elinav E, Huber S, Booth CJ, Strowig T, Jin C, Eisenbarth SC, Flavell RA. Inflammation-induced tumorigenesis in the colon is regulated by caspase-1 and NLRC4. Proc Natl Acad Sci USA. 2010; 107:21635–21640. [PubMed: 21118981]

Hu Z, Zhou Q, Zhang C, Fan S, Cheng W, Zhao Y, Shao F, Wang HW, Sui SF, Chai J. Structural and biochemical basis for induced self-propagation of NLRC4. Science. 2015; 350:399–404. [PubMed: 26449475]

Karki R, Man SM, Malireddi RKS, Gurung P, Vogel P, Lamkanfi M, Kanneganti TD. Concerted activation of the AIM2 and NLRP3 inflammasomes orchestrates host protection against Aspergillus infection. Cell Host Microbe. 2015; 17:357–368. [PubMed: 25704009]

Kayagaki N, Stowe IB, Lee BL, O'Rourke K, Anderson K, Warming S, Cuellar T, Haley B, Roose-Girma M, Phung QT, et al. Caspase-11 cleaves gasdermin D for non-canonical inflammasome signalling. Nature. 2015; 526:666–671. [PubMed: 26375259]

Knodler LA, Crowley SM, Sham HP, Yang H, Wrande M, Ma C, Ernst RK, Steele-Mortimer O, Celli J, Vallance BA. Noncanonical inflammasome activation of caspase-4/caspase-11 mediates epithelial defenses against enteric bacterial pathogens. Cell Host Microbe. 2014; 16:249–256. [PubMed: 25121752]

Knodler LA, Vallance BA, Celli J, Winfree S, Hansen B, Montero M, Steele-Mortimer O. Dissemination of invasive Salmonella via bacterial-induced extrusion of mucosal epithelia. Proc Natl Acad Sci USA. 2010; 107:17733–17738. [PubMed: 20876119]

Kofoed EM, Vance RE. Innate immune recognition of bacterial ligands by NAIPs determines inflammasome specificity. Nature. 2011; 477:592–595. [PubMed: 21874021]

Author Manuscript Author Manuscript Author Manuscript Author Manuscript

Lamkanfi M, Dixit VM. Mechanisms and functions of inflammasomes. Cell. 2014; 157:1013–1022. [PubMed: 24855941]

Lara-Tejero M, Sutterwala FS, Ogura Y, Grant EP, Bertin J, Coyle AJ, Flavell RA, Galán JE. Role of the caspase-1 inflammasome in Salmonella typhimurium pathogenesis. J Exp Med. 2006; 203:1407–1412. [PubMed: 16717117]

LaRock CN, Cookson BT. Burning down the house: cellular actions during pyroptosis. PLoS Pathog. 2013; 9:e1003793. [PubMed: 24367258]

Levy M, Thaiss CA, Zeevi D, Dohnalová L, Zilberman-Schapira G, Mahdi JA, David E, Savidor A, Korem T, Herzig Y, et al. Microbiota-Modulated Metabolites Shape the Intestinal Microenvironment by Regulating NLRP6 Inflammasome Signaling. Cell. 2015; 163:1428–1443. [PubMed: 26638072]

Li P, Allen H, Banerjee S, Franklin S, Herzog L, Johnston C, McDowell J, Paskind M, Rodman L, Salfeld J. Mice deficient in IL-1 beta-converting enzyme are defective in production of mature IL-1 beta and resistant to endotoxic shock. Cell. 1995; 80:401–411. [PubMed: 7859282]

Man SM, Tourlomousis P, Hopkins L, Monie TP, Fitzgerald KA, Bryant CE. Salmonella infection induces recruitment of Caspase-8 to the inflammasome to modulate IL-1β production. J Immunol. 2013; 191:5239–5246. [PubMed: 24123685]

Mariathasan S, Newton K, Monack DM, Vucic D, French DM, Lee WP, Roose-Girma M, Erickson S, Dixit VM. Differential activation of the inflammasome by caspase-1 adaptors ASC and Ipaf. Nature. 2004; 430:213–218. [PubMed: 15190255]

Masumoto J, Dowds TA, Schaner P, Chen FF, Ogura Y, Li M, Zhu L, Katsuyama T, Sagara J, Taniguchi S, et al. ASC is an activating adaptor for NF-kappa B and caspase-8-dependent apoptosis. Biochemical and Biophysical Research Communications. 2003; 303(1):69–73. [PubMed: 12646168]

Miao EA, Leaf IA, Treuting PM, Mao DP, Dors M, Sarkar A, Warren SE, Wewers MD, Aderem A. Caspase-1-induced pyroptosis is an innate immune effector mechanism against intracellular bacteria. Nat Immunol. 2010; 11:1136–1142. [PubMed: 21057511]

Miyoshi H, Stappenbeck TS. In vitro expansion and genetic modification of gastrointestinal stem cells in spheroid culture. Nat Protoc. 2013; 8:2471–2482. [PubMed: 24232249]

von Moltke J, Trinidad NJ, Moayeri M, Kintzer AF, Wang SB, van Rooijen N, Brown CR, Krantz BA, Leppla SH, Gronert K, et al. Rapid induction of inflammatory lipid mediators by the inflammasome in vivo. Nature. 2012; 490:107–111. [PubMed: 22902502]

Müller AA, Dolowschiak T, Sellin ME, Felmy B, Verbree C, Gadient S, Westermann AJ, Vogel J, LeibundGut-Landmann S, Hardt WD. An NK Cell Perforin Response Elicited via IL-18 Controls Mucosal Inflammation Kinetics during Salmonella Gut Infection. PLoS Pathog. 2016; 12:e1005723. [PubMed: 27341123]

Nordlander S, Pott J, Maloy KJ. NLRC4 expression in intestinal epithelial cells mediates protection against an enteric pathogen. Mucosal Immunol. 2013

Rauch I, Tenthorey JL, Nichols RD, Al Moussawi K, Kang JJ, Kang C, Kazmierczak BI, Vance RE. NAIP proteins are required for cytosolic detection of specific bacterial ligands in vivo. J Exp Med. 2016; 213:657–665. [PubMed: 27045008]

Romberg N, Al Moussawi K, Nelson-Williams C, Stiegler AL, Loring E, Choi M, Overton J, Meffre E, Khokha MK, Huttner AJ, et al. Mutation of NLRC4 causes a syndrome of enterocolitis and autoinflammation. Nat Genet. 2014; 46:1135–1139. [PubMed: 25217960]

Rosenblatt J, Raff MC, Cramer LP. An epithelial cell destined for apoptosis signals its neighbors to extrude it by an actin- and myosin-dependent mechanism. Curr Biol. 2001; 11:1847–1857. [PubMed: 11728307]

Sasaki Y, Derudder E, Hobeika E, Pelanda R, Reth M, Rajewsky K, Schmidt-Supprian M. Canonical NF-kappaB activity, dispensable for B cell development, replaces BAFF-receptor signals and promotes B cell proliferation upon activation. Immunity. 2006; 24:729–739. [PubMed: 16782029]

Sato T, Clevers H. Primary mouse small intestinal epithelial cell cultures. Methods Mol Biol. 2013; 945:319–328. [PubMed: 23097115]

Sellin ME, Maslowski KM, Maloy KJ, Hardt WD. Inflammasomes of the intestinal epithelium. Trends Immunol. 2015; 36:442–450. [PubMed: 26166583]

Author Manuscript Author Manuscript Author Manuscript Author Manuscript

Sellin ME, Müller AA, Felmy B, Dolowschiak T, Diard M, Tardivel A, Maslowski KM, Hardt WD. Epithelium-intrinsic NAIP/NLRC4 inflammasome drives infected enterocyte expulsion to restrict Salmonella replication in the intestinal mucosa. Cell Host Microbe. 2014; 16:237–248. [PubMed: 25121751]

Shi J, Zhao Y, Wang K, Shi X, Wang Y, Huang H, Zhuang Y, Cai T, Wang F, Shao F. Cleavage of GSDMD by inflammatory caspases determines pyroptotic cell death. Nature. 2015; 526:660–665. [PubMed: 26375003]

Srinivas S, Watanabe T, Lin CS, William CM, Tanabe Y, Jessell TM, Costantini F. Cre reporter strains produced by targeted insertion of EYFP and ECFP into the ROSA26 locus. BMC Dev Biol. 2001; 1:4. [PubMed: 11299042]

Strowig T, Henao-Mejia J, Elinav E, Flavell R. Inflammasomes in health and disease. Nature. 2012; 481:278–286. [PubMed: 22258606]

Wang H, Yang H, Shivalila CS, Dawlaty MM, Cheng AW, Zhang F, Jaenisch R. One-Step Generation of Mice Carrying Mutations in Multiple Genes by CRISPR/Cas-Mediated Genome Engineering. Cell. 2013; 153:910–918. [PubMed: 23643243]

Wlodarska M, Thaiss CA, Nowarski R, Henao-Mejia J, Zhang JP, Brown EM, Frankel G, Levy M, Katz MN, Philbrick WM, et al. NLRP6 Inflammasome Orchestrates the Colonic Host-Microbial Interface by Regulating Goblet Cell Mucus Secretion. Cell. 2014; 156:1045–1059. [PubMed: 24581500]

Zhang L, Chen S, Ruan J, Wu J, Tong AB, Yin Q, Li Y, David L, Lu A, Wang WL, et al. Cryo-EM structure of the activated NAIP2-NLRC4 inflammasome reveals nucleated polymerization. Science. 2015; 350:404–409. [PubMed: 26449474]

Zhao Y, Yang J, Shi J, Gong YN, Lu Q, Xu H, Liu L, Shao F. The NLRC4 inflammasome receptors for bacterial flagellin and type III secretion apparatus. Nature. 2011; 477:596–600. [PubMed: 21918512]

Author Manuscript Author Manuscript Author Manuscript Author Manuscript

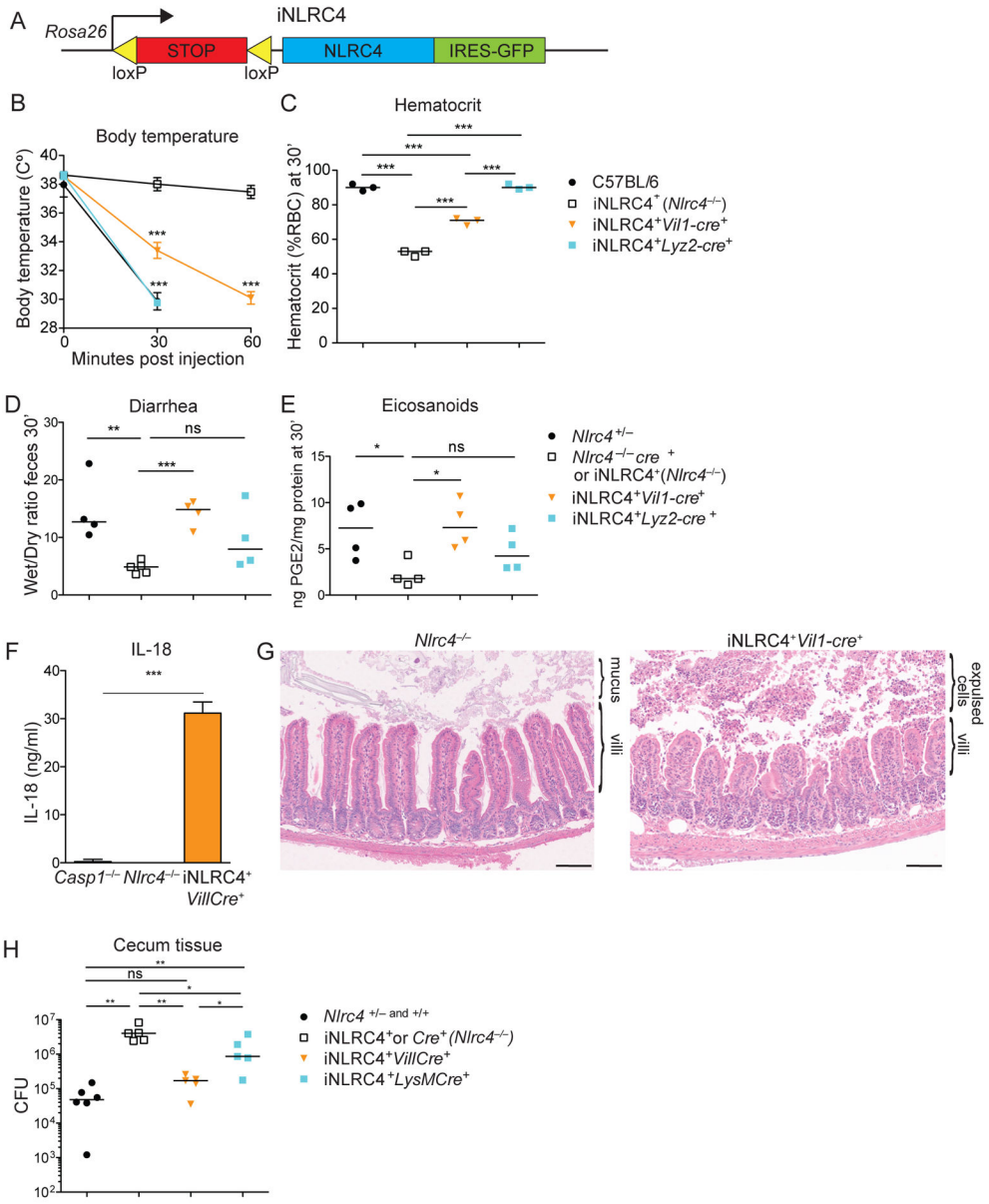

Figure 1. Specific activation of NLRC4 in intestinal epithelial cells protects from pathogen invasion but can lead to intestinal pathology

(**A**) Schematic of the *Rosa26* locus after successful gene targeting with iNLRC4-IRES-GFP. Yellow triangles represent LoxP sites. (**B, C**) Mice were injected with 0.8μg/g PA and 0.4μg/g LFn-Fla and monitored for (B) body temperature and (C) hematocrit (30 minutes, n=3). (**D, E**) Mice were injected with 0.8μg/g PA and 80ng/g LFn-Fla166 and (D) wet/dry ratio of intestinal content and (E) PGE_2 amounts of intestinal tissue from mice treated for 30 minutes were determined (n=4–5). (**F**) Quantification of serum IL-18 using ELISA in mice treated as in B), 60 minute timepoint (n=3). (**G**) H&E staining of small intestinal tissue from mice treated as in B), 60 minutes post injection. Scale bar = 100μm (**H**) CFU in cecum 18h after oral *S.*Typhimurium infection (n=5). Data are representative of 3 independent experiments. (B,F) mean± SD, (C–E,H) median, (B–E) unpaired t-test (in B compared to

Author Manuscript Author Manuscript Author Manuscript Author Manuscript

Nlrc4$^{-/-}$), (H) Mann-Whitney test, *p<0.01, **p<0.005, ***p<0.001. Please see also Figure S1

Author Manuscript Author Manuscript Author Manuscript Author Manuscript

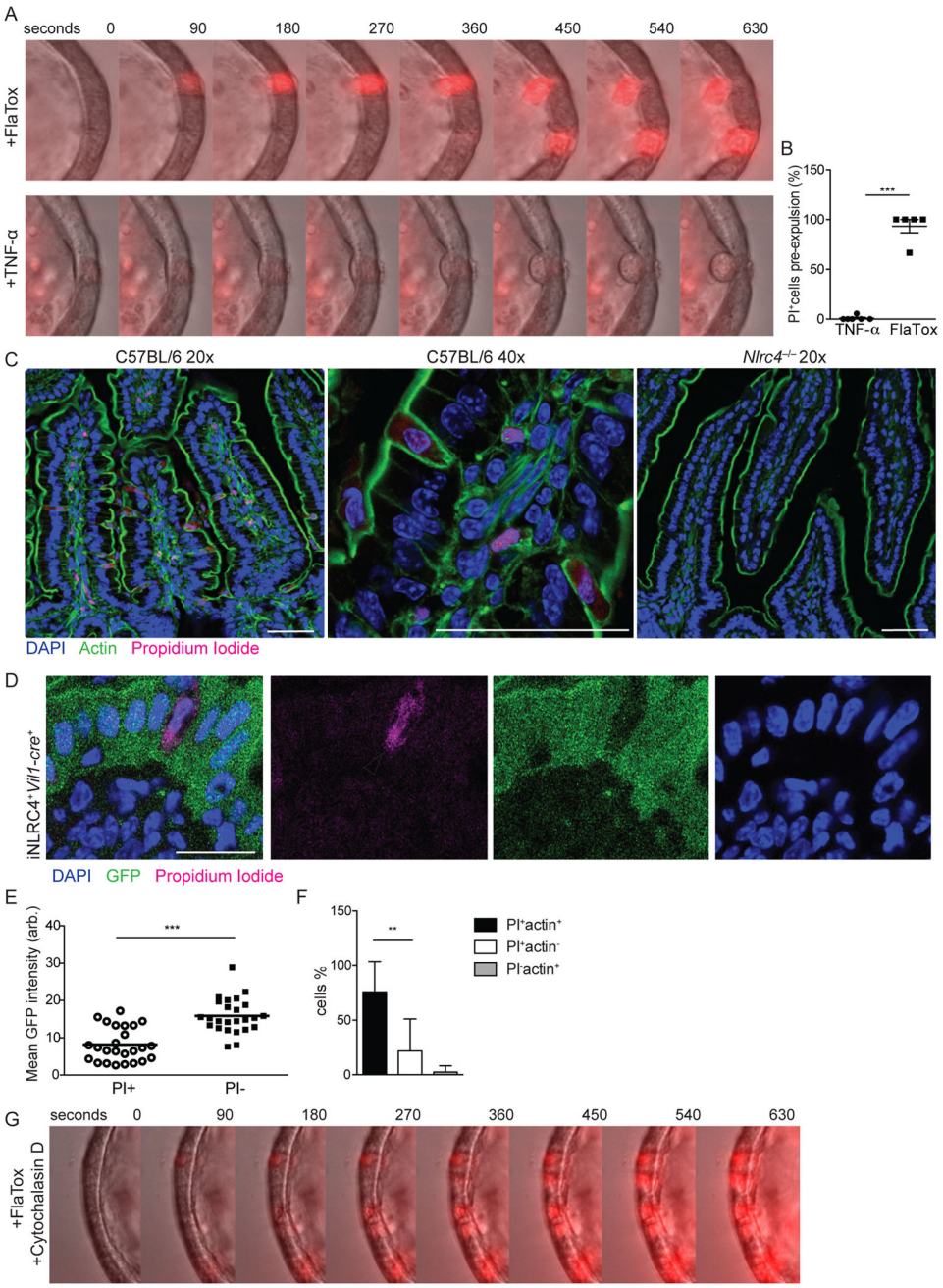

Figure 2. Cell autonomous expulsion and lytic death of IECs

(**A**) Wild-type small intestinal organoid treated with 16μg/ml of PA and 1μg/ml LFn-Fla166 (upper lane) or 100ng/ml TNF-α (lower lane) and stained with propidium iodide. (**B**) Blinded quantification of C57BL/6 small intestinal organoid cells positive for propidium iodide before expulsion in Fla166Tox vs. TNF-α treatment as in A). n=5–6 movies/ treatment. (**C**) Propidium iodide and fluorescent phalloidin (actin) or (**D**) Propidium iodide and GFP in small intestines from mice treated with 0.2μg/g of PA and 0.1μg/g LFn-Fla for 60 minutes. Arrows indicate expulsing cells. Scale bar = 40 (C) 20 (D) μm (**E**) Quantification of GFP signal in propidium iodide positive and neighboring negative cells

Author Manuscript Author Manuscript Author Manuscript Author Manuscript

from samples as in (D) (n=3). (**F**) Quantification of actin purse strings in propidium iodide positive cells from samples as in (C) (n=7) (**G**) Wild-type small intestinal organoid treated with 16μg/ml of PA, 1μg/ml LFn-Fla166 and 2.5μM cytochalasin D and stained with propidium iodide. Data representative of at least 2 independent experiments, unpaired t-test, **p<0.005, ***p<0.001. Please see also Figure S2

Author Manuscript Author Manuscript Author Manuscript Author Manuscript

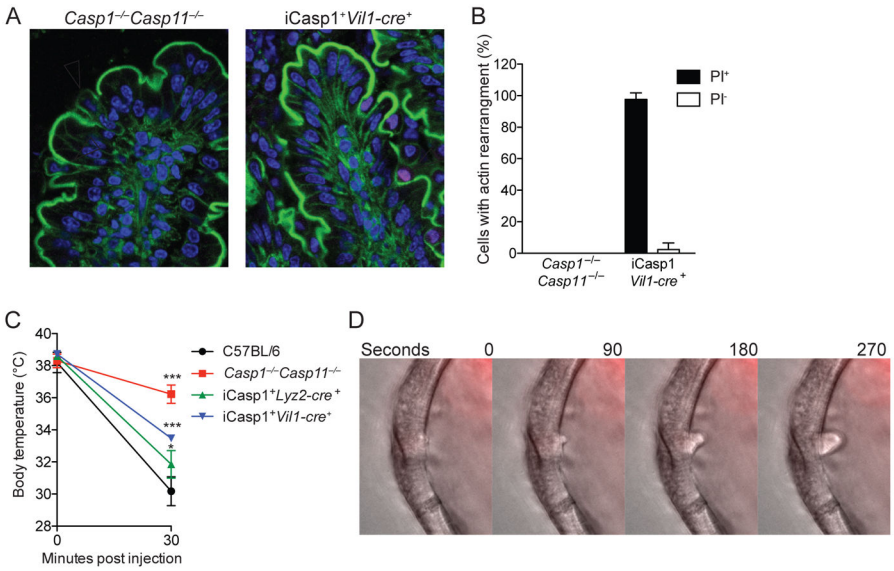

Figure 3. Caspase-1 is required for IEC pyroptosis but not IEC expulsion

(**A**) Propidium iodide and fluorescent phalloidin (actin) in small intestines from mice treated with 0.8μg/g PA and 0.4μg/g LFn-Fla for 60 minutes. Arrows indicate expulsing cells. Scale bar = 20μm (**B**) Blinded quantification of propidium iodide positive and negative cells with actin purse strings in samples as in (A) (n=3) (**C**) Mice were treated as in (A) and monitored for body temperature (n=3). (**D**) *Casp1*$^{-/-}$ small intestinal organoid treated with 16μg/ml of PA and 1μg/ml LFn-Fla166 and stained with propidium iodide. Data representative of at least 2 independent experiments. (B, C): mean± SD, (C) unpaired t-test compared to *Casp1*$^{-/-}$*Casp11*$^{-/-}$, ***p<0.001. Please see also Figure S3

Author Manuscript Author Manuscript Author Manuscript Author Manuscript

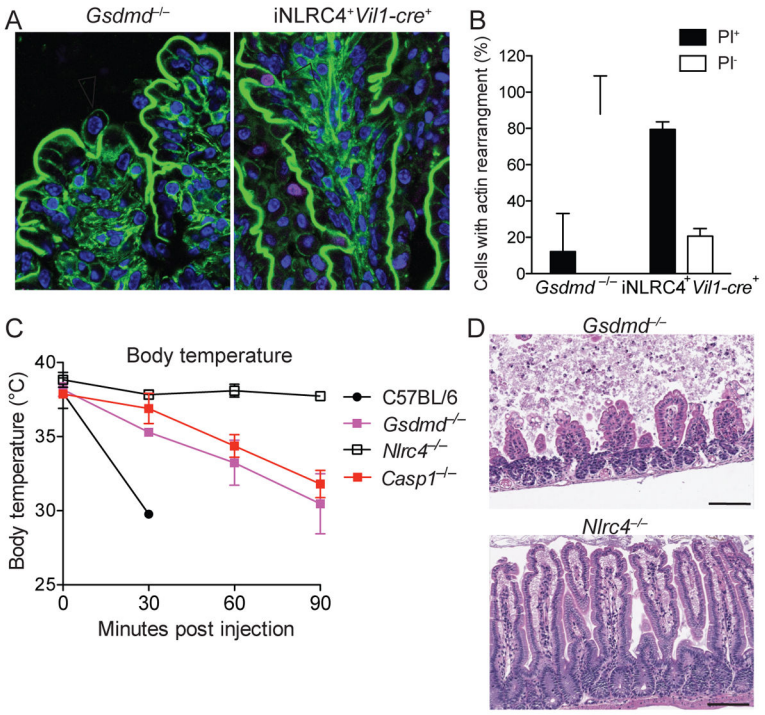

Figure 4. Gasdermin D is required for IEC pyroptosis but not IEC expulsion

(**A**) Propidium iodide and fluorescent phalloidin (actin) in small intestines from mice treated with 0.8μg/g PA and 0.4μg/g LFn-Fla for 60 minutes. Arrows indicate expulsing cells. Scale bar = 20μm (**B**) Blinded quantification of propidium iodide positive and negative cells with actin purse strings in samples as in (A) (n=3) (**C**) Mice were injected with 0.8μg/g PA and 0.4μg/g LFn-Fla and monitored for body temperature (n=3). (**D**) H&E staining of small intestinal tissue from mice treated as in A, 90 minute timepoint. Scale bar = 100μm Data representative of at least 2 independent experiments. (B, C): mean± SD, (C) unpaired t-test compared to *Nlrc4*$^{-/-}$,**p<0.005, ***p<0.001. Please see also Figure S4

Author Manuscript Author Manuscript Author Manuscript Author Manuscript

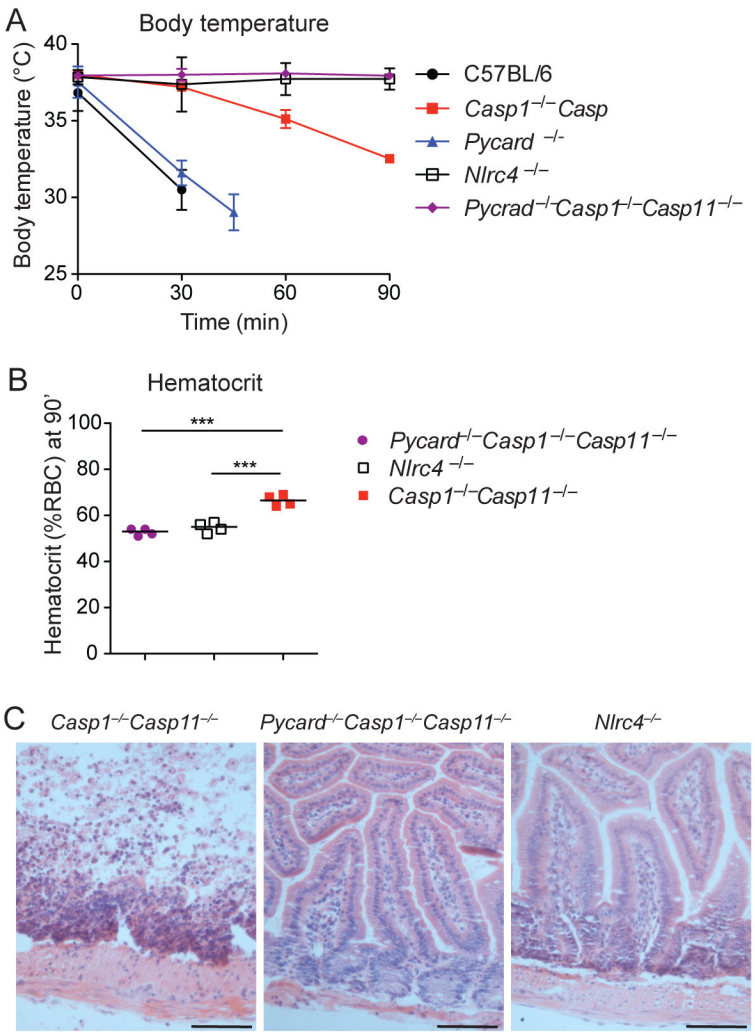

Figure 5. ASC is required for the Caspase1-independent NLRC4 signaling

(**A, B**) Mice were injected with 0.8μg/g PA and 0.4μg/g LFn-Fla and monitored for (A) body temperature and (B) hematocrit (90 minutes, n=3). (**C**) H&E staining of small intestinal tissue from mice treated as in (A), 90 minute timepoint. Scale bar = 100μm Data representative of 2 independent experiments. (A): mean± SD, (B): median. unpaired t-test (in A compared to *Nlrc4*$^{-/-}$), **p<0.005, ***p<0.001. Please see also Figure S3

Author Manuscript Author Manuscript Author Manuscript Author Manuscript

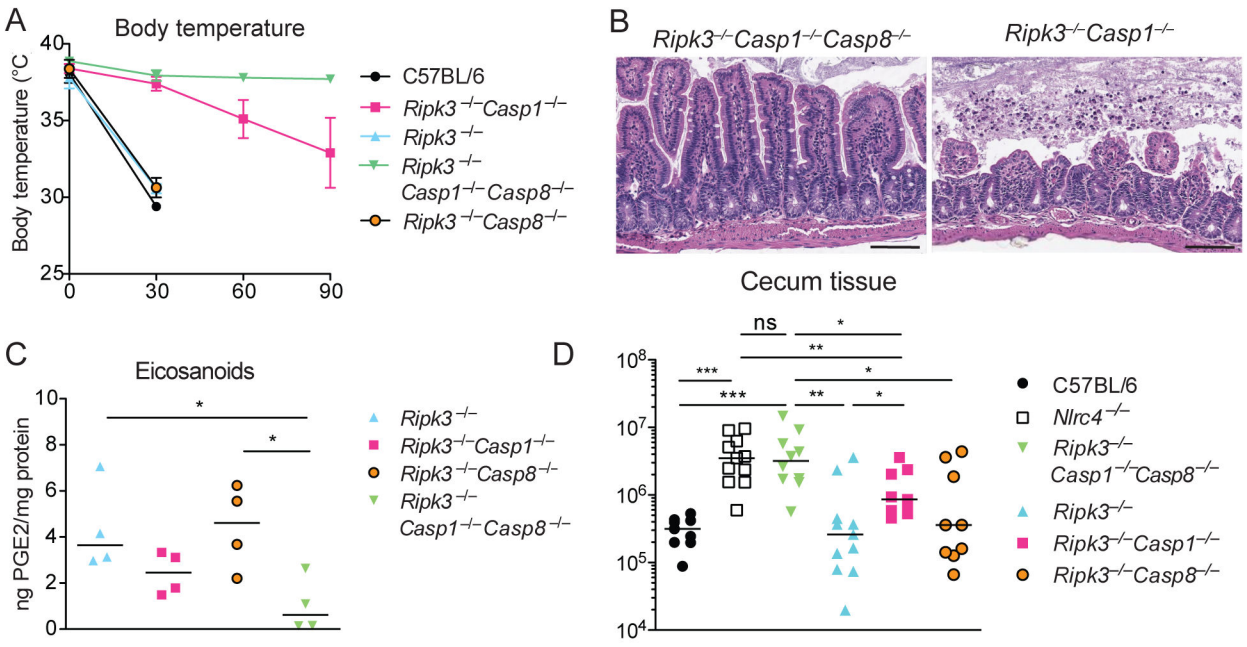

Figure 6. A Caspase 8 inflammasome compensates for loss of Caspase 1

(**A**) Mice were injected with 0.8μg/g PA and 0.4μg/g LFn-Fla and monitored for body temperature (n=3), mean± SD. (**B**) H&E staining of small intestinal tissue from mice treated as in (A), 90 minute timepoint. Scale bar = 100μm (**C**) PGE_2 lamounts of intestinal tissue from mice treated as in (A) for 30 minutes were determined (n=4/group), median. Data representative of 2 independent experiments. (**D**) CFU in cecum 18h after oral *S.*Typhimurium infection (n=10), combined data of 2 independent experiments. (A+C) unpaired t-test (in A compared to *Ripk3*$^{-/-}$*Casp1*$^{-/-}$*Casp8*$^{-/-}$). (D) Mann-Whitney test, *p<0.01, **p<0.005, ***p<0.001. Please see also Figure S5+6